

Polarimetry by classical ghost diffraction

Henri Kellock^{1,*}, Tero Setälä¹, Ari T. Friberg¹, and Tomohiro Shirai²

¹*Institute of Photonics, University of Eastern Finland, P.O. Box 111, FI-80101 Joensuu, Finland*

²*Research Institute of Instrumentation Frontier, National Institute of Advanced Industrial Science and Technology, AIST Tsukuba Central 2, 1-1-1 Umezono, Tsukuba 305-8568, Japan*

We present a technique for studying the polarimetric properties of a birefringent object by means of classical ghost diffraction. The standard ghost diffraction setup is modified to include polarizers for controlling the state of polarization of the beam in various places. The object is characterized by a Jones matrix and the absolute values of the Fourier transforms of its individual elements are measured. From these measurements the original complex-valued functions can be retrieved through iterative methods resulting in the full Jones matrix of the object. We present two different placements of the polarizers and show that one of them leads to better polarimetric quality, while the other placement offers the possibility to perform polarimetry without controlling the source's state of polarization. The concept of an effective source is introduced to simplify the calculations. Ghost polarimetry enables the assessment of polarization properties as a function of position within the object through simple intensity correlation measurements.

I. INTRODUCTION

Ghost imaging, or correlation imaging, is an imaging technique where quantum entanglement and photon coincidences or classical intensity correlation statistics are used to provide information on an object through indirect measurements [1, 2]. Setups can be arranged to form either the image or the far-field diffraction pattern of the object. The classical counterpart of ghost imaging has its merits in readily-available and cost-effective, bright light sources. It is able to emulate most aspects of quantum ghost imaging [3–8], although classical correlation imaging has limitations with regard to the visibility (contrast) of the resulting image [9–11]. Techniques have been developed to overcome these limitations, including higher-order correlations [9, 11], background subtraction [10], differential ghost imaging [12] and computational ghost imaging [13, 14]. Using electromagnetic theory also the effects that the degree of polarization of the light has on correlation imaging have been studied recently [11, 15–17].

In this paper we introduce a method for obtaining the polarimetric properties of a (partially) transparent, spatially dependent, arbitrarily birefringent or dichroic object by means of correlation imaging. In contrast to quantum ellipsometry with two-photon polarization-entangled light in reflection geometry reported previously [18–20], we consider light from a classical, spatially incoherent, partially polarized source interacting with the object in transmission arrangement. We make use of electromagnetic theory of optical coherence and employ a modified ghost diffraction setup, with the concept of an effective source used for convenience of analysis. Whereas elaborate techniques for measuring an object's polarization properties based on Mueller imaging and Stokes imaging have been developed [21], in many

applications (such as thin-film optics and nanophotonics) a simpler polarimetric characterization of the object by means of its Jones matrix is adequate. The conventional way of measuring the Jones matrix of a spatially uniform, planar object makes use of a coherent laser, two polarizers and a detector [21]. In correlation imaging light from a spatially incoherent source is split into two arms, a test arm containing the object followed by a non-resolving detector and a reference arm with a CCD camera. The intensities recorded at the end of the two arms are correlated to obtain either the image or the far-field diffraction pattern of the object. For polarimetry by ghost diffraction we present two possible arrangements. In one, polarizers are placed after the source and before the detectors. In the other arrangement the source's state of polarization is not controlled and the polarizers are located in front of the detectors in each arm. In both cases measurements are done with different orientations of the polarizers to individually select all the elements of the object's Jones matrix. The advantage of ghost polarimetry is that spatially varying, polarization-state altering objects can be analyzed.

Section II recalls briefly the Jones calculus and the conventional measurement of the Jones matrix components. In section III we introduce the mathematical notion of the effective source and incorporate it in our discussion on electromagnetic ghost diffraction. In section IV the standard ghost diffraction setup is modified in two different ways so as to enable the measurement of the polarimetric properties of an unknown object. The polarimetric qualities of these two setups are assessed in terms of image visibility. The main conclusions are summarized in section V. Appendix A gives further details on the possible placements of the polarizers and on the constraints the placements put upon the source.

* henri.kellock@uef.fi

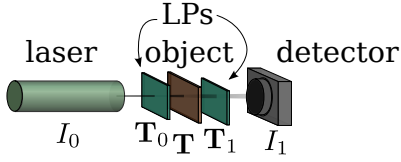


Figure 1. Measuring the elements of the matrix \mathbf{T} that describes the response of the object. The setup consists of a spatially coherent laser source (I_0), the object which is placed between two linear polarizers (LPs), \mathbf{T}_0 and \mathbf{T}_1 , and a detector. The measured intensity (I_1) is compared to the case where the object and the second LP are removed.

II. JONES FORMALISM FOR POLARIMETRY

We employ spectral electromagnetic coherence theory to analyze polarimetry by ghost diffraction. A realization of a random, beam-like electric field at position \mathbf{r} and frequency ω , propagating in the z direction is denoted by $\mathbf{E}(\mathbf{r}) = [E_x(\mathbf{r}) E_y(\mathbf{r})]^T$, where the superscript T denotes the transpose and the frequency dependence is suppressed for brevity. On illuminating with a linear, polarimetric (birefringent, dichroic), planar optical element $\mathbf{T}(\mathbf{r})$ the output electric field $\mathbf{E}_{\text{out}}(\mathbf{r})$ is related to the input electric field $\mathbf{E}_{\text{in}}(\mathbf{r})$ through [22]

$$\mathbf{E}_{\text{out}}(\mathbf{r}) = \mathbf{T}(\mathbf{r})\mathbf{E}_{\text{in}}(\mathbf{r}), \quad (1)$$

where

$$\mathbf{T}(\mathbf{r}) = \begin{bmatrix} T_{xx}(\mathbf{r}) & T_{xy}(\mathbf{r}) \\ T_{yx}(\mathbf{r}) & T_{yy}(\mathbf{r}) \end{bmatrix} \quad (2)$$

is the optical element's transmission (or Jones) matrix. We take $T_{ij} \in \mathbb{C}$ with $i, j \in \{x, y\}$ to be deterministic and, in general, spatially dependent when \mathbf{T} represents the object. For polarizers (and wave plates) the elements of \mathbf{T} are constant. For example,

$$\mathbf{T}^x = \begin{bmatrix} 1 & 0 \\ 0 & 0 \end{bmatrix}, \quad \mathbf{T}^y = \begin{bmatrix} 0 & 0 \\ 0 & 1 \end{bmatrix} \quad (3)$$

are uniform linear polarizers (LPs) that only let the x or y component of the light go through, unaltered.

The conventional way to determine the polarimetric response of an unknown optical element is to measure the components of the corresponding Jones matrix \mathbf{T} individually. Normally, for a uniform object, this is done with a setup schematically depicted in figure 1. A spatially coherent, uniformly polarized, monochromatic laser beam illuminates the object which is sandwiched between two LPs, the 'polarizer' \mathbf{T}_0 and the 'analyzer' \mathbf{T}_1 and the transmitted intensity is recorded with a detector. To avoid effects of diffraction, the elements \mathbf{T}_0 and \mathbf{T}_1 and the detector are deep in the Fresnel zone of the object \mathbf{T} . According to equation (1) the field \mathbf{E}_1 at the detector is described by

$$\mathbf{E}_1 = \mathbf{T}_1 \mathbf{T} \mathbf{T}_0 \mathbf{E}_0, \quad (4)$$

where \mathbf{E}_0 is the coherent electric field of the laser source. Orientating the LPs so that $\mathbf{T}_0 = \mathbf{T}^i$ and $\mathbf{T}_1 = \mathbf{T}^j$, with $i, j \in \{x, y\}$, we obtain, from equations (3) and (4), the intensity

$$I_1 = \mathbf{E}_1^\dagger \mathbf{E}_1 = |T_{ji}|^2 |E_{0,i}|^2, \quad (5)$$

where the dagger denotes the Hermitian conjugate and $|E_{0,i}|^2 = I_{0,i}$ are the intensities of the source components. These can be measured by removing \mathbf{T} and \mathbf{T}_1 from the setup and varying \mathbf{T}_0 . Hence we can calculate $|T_{ji}|$ with all $i, j \in \{x, y\}$.

Equation (5) demonstrates that only the absolute values $|T_{ij}|$ of the object's Jones matrix are obtained with this method. Using a considerably more complicated system one could measure all the complex transmission matrix parameters T_{ij} of a spatially independent object. Such a setup involves linear polarizers oriented at ± 45 degrees with respect to the x axis as well as circular polarizers in addition to the LPs introduced earlier [21]. If the object has spatial dependence, the detector in figure 1 may in principle be replaced with a CCD array.

III. GHOST DIFFRACTION

After more than a decade of research, ghost imaging and diffraction are now well-established optical techniques [1, 2]. In particular, lensless ghost diffraction is employed to obtain the far-field pattern, or the Fourier transform, of the object [23–25]. Classical ghost imaging and diffraction are conveniently analyzed using optical coherence theory [26, 27]. In what follows we introduce also the novel idea of an 'effective source' which greatly simplifies the calculations.

A. Intensity and field correlations

We need to compute the correlations between the intensities in the two arms of the ghost diffraction setup, i.e., the intensities $I_\alpha = \mathbf{E}_\alpha^\dagger \mathbf{E}_\alpha$ with $\alpha \in \{1, 2\}$. Besides the frequency ω , in this section we further suppress the spatial dependencies of the functions for notational brevity. We begin by dividing I_α into the intensities of the x and y components of the electric field as $I_\alpha = I_{\alpha,x} + I_{\alpha,y}$. The intensity correlation can then be expressed as

$$\langle I_1 I_2 \rangle = \sum_{i,j \in \{x,y\}} \langle I_{1,i} I_{2,j} \rangle, \quad (6)$$

where $\langle \dots \rangle$ denotes the ensemble average. Assuming that the field fluctuations of the source obey Gaussian statistics, we may use the Gaussian moment theorem to write $\langle I_{1,i} I_{2,j} \rangle$ in terms of second-order field correlations as [11, 15, 16, 28]

$$\langle I_{1,i} I_{2,j} \rangle = W_{11,ii} W_{22,jj} + |W_{12,ij}|^2, \quad (7)$$

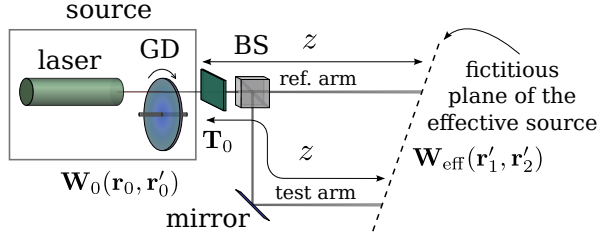


Figure 2. Concept of the effective source. A laser and a rotating ground glass disk (GD) create a spatially incoherent planar field. The polarizer \mathbf{T}_0 , controlling the state of polarization of the source, may or may not exist before the beam splitter (BS) which directs the light into the reference arm and the test arm. The beams propagate over the distance z in both arms until reaching the fictitious plane of the effective source.

where $W_{\alpha\beta,ij} = \langle E_{\alpha,i}^* E_{\beta,j} \rangle$, $\alpha, \beta \in \{1, 2\}$, $i, j \in \{x, y\}$, is the cross-spectral density function and $E_{\alpha,i}$ denotes the i component of the field in arm α .

Combining equations (6) and (7) and making use of the cross-spectral density matrix (CSDM)

$$\mathbf{W}_{\alpha\beta} = \begin{bmatrix} W_{\alpha\beta,xx} & W_{\alpha\beta,xy} \\ W_{\alpha\beta,yx} & W_{\alpha\beta,yy} \end{bmatrix}, \quad (8)$$

we can write the intensity correlation in a compact form as [11, 17]

$$\langle I_1 I_2 \rangle = \text{tr} \mathbf{W}_{11} \text{tr} \mathbf{W}_{22} + \text{tr} \mathbf{W}_{12}^\dagger \mathbf{W}_{12}, \quad (9)$$

where tr denotes the trace, $\text{tr} \mathbf{W}_{\alpha\alpha} = \langle I_\alpha \rangle$ is the average intensity in the α th arm and $\text{tr} \mathbf{W}_{12}^\dagger \mathbf{W}_{12} = \langle \Delta I_1 \Delta I_2 \rangle$ is the correlation of the intensity fluctuations $\Delta I_\alpha \equiv I_\alpha - \langle I_\alpha \rangle$ between the two different arms.

B. Effective source

Before proceeding into the technical details of ghost diffraction, we present with reference to figure 2 the notion of the effective source. Coherent laser radiation passed through a rotating disk of ground glass generates a stationary, uniformly polarized, spatially incoherent beam of light characterized by the cross-spectral density matrix $\mathbf{W}_0(\mathbf{r}_0, \mathbf{r}'_0)$. We then consider two possibilities: behind the physical source there may be a linear polarizer represented by the matrix \mathbf{T}_0 , or it may be absent. A beam splitter separates the field into the reference and test paths, followed by propagation over an equal distance z in each arm. The light characterized by the CSDM $\mathbf{W}_{\text{eff}}(\mathbf{r}'_1, \mathbf{r}'_2)$ in the ensuing fictitious plane constitutes the effective source.

Within the accuracy of Fresnel diffraction, the effective source's CSDM is given by (see figure 2)

$$\mathbf{W}_{\text{eff}}(\mathbf{r}'_1, \mathbf{r}'_2) = \iint_{-\infty}^{\infty} d^2 r_0 d^2 r'_0 \mathbf{W}(\mathbf{r}_0, \mathbf{r}'_0) K_1^*(\mathbf{r}_0, \mathbf{r}'_1) K_2(\mathbf{r}'_0, \mathbf{r}'_2) \quad (10)$$

where $\mathbf{W}(\mathbf{r}_0, \mathbf{r}'_0) = \mathbf{W}_0(\mathbf{r}_0, \mathbf{r}'_0)$ in the absence of the polarizer \mathbf{T}_0 and $\mathbf{W}(\mathbf{r}_0, \mathbf{r}'_0) = \mathbf{T}_0^* \mathbf{W}_0(\mathbf{r}_0, \mathbf{r}'_0) \mathbf{T}_0^\dagger$ in the presence of \mathbf{T}_0 . Further, the kernel [26, 29]

$$K_\alpha(\mathbf{r}_0, \mathbf{r}'_\alpha) = \frac{-ik}{2\pi z} \exp \left[\frac{ik}{2z} (\mathbf{r}'_\alpha - \mathbf{r}_0)^2 \right], \quad (11)$$

with $\alpha \in \{1, 2\}$ and $k = \omega/c$ being the wave number (c is the vacuum speed of light), describes field propagation over the distance z in free space from the physical source plane to the fictitious plane of the effective source.

Now, in classical ghost diffraction the actual source is spatially completely incoherent. Hence we may take $\mathbf{W}_0(\mathbf{r}_0, \mathbf{r}'_0) = \mathbf{J}_0 \delta(\mathbf{r}'_0 - \mathbf{r}_0)$, where \mathbf{J}_0 is the polarization matrix of the source and $\delta(\mathbf{r})$ is the two-dimensional Dirac delta function. Applying the δ function to eliminate \mathbf{r}'_0 and using equation (11), equation (10) then becomes

$$\mathbf{W}_{\text{eff}}(\mathbf{r}'_1, \mathbf{r}'_2) = \mathbf{J}_{\text{eff}} \delta(\mathbf{r}'_2 - \mathbf{r}'_1), \quad (12)$$

where $\mathbf{J}_{\text{eff}} = \mathbf{T}_0^* \mathbf{J}_0 \mathbf{T}_0^\dagger$ with \mathbf{T}_0 and $\mathbf{J}_{\text{eff}} = \mathbf{J}_0$ without \mathbf{T}_0 . Equation (12) shows that in the case of a (sufficiently wide) spatially completely incoherent physical source also the effective source is spatially incoherent.

C. Fourier transform by ghost diffraction

We next demonstrate that in the context of classical ghost diffraction the concept of the effective source is consistent with the formation of the Fourier transform of the object distribution. We represent the object here as $\mathbf{T}(\mathbf{r}') = T(\mathbf{r}') \mathbf{I}$, where \mathbf{I} is the 2×2 unit matrix and omit the polarizer \mathbf{T}_0 that controls the source's polarization

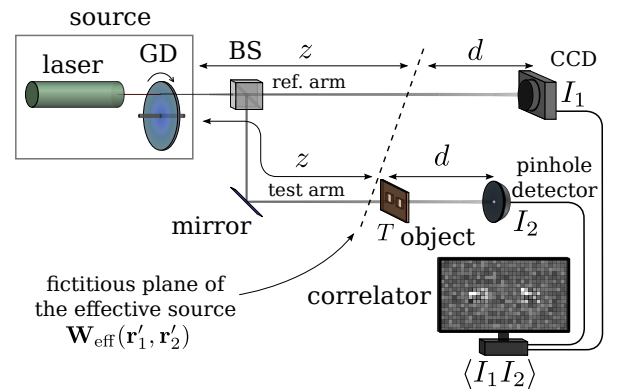


Figure 3. Effective source in ghost diffraction. The fictitious plane is at a distance z from the true source and contains the effective source characterized by $\mathbf{W}_{\text{eff}}(\mathbf{r}'_1, \mathbf{r}'_2)$ (see figure 2). In the reference arm the wave propagates a further distance d and is detected by a CCD camera. In the test arm the object T is located immediately after the effective source and the field then travels the same distance d onto a pinhole detector. The measured intensities I_1 and I_2 are correlated.

state, as is illustrated in figure 3. In the test arm the object is placed immediately after the effective source. The fields then propagate from the effective source plane an equal distance d in both arms to the detectors, which are taken to be pointlike.

Using an expression of the form of equation (10) with integrations over the effective source, we obtain for the CSDM between the electric fields in the two arms the formula

$$\mathbf{W}_{12}(\mathbf{r}_1, \mathbf{r}_2) = \iint_{-\infty}^{\infty} d^2r'_1 d^2r'_2 \mathbf{W}_{\text{eff}}(\mathbf{r}'_1, \mathbf{r}'_2) \times T(\mathbf{r}'_2) K_1^*(\mathbf{r}'_1, \mathbf{r}_1) K_2(\mathbf{r}'_2, \mathbf{r}_2), \quad (13)$$

where $T(\mathbf{r}'_2)$ is the object's transmission function. On further employing equations (11) and (12) with $z = d$ and $\mathbf{J}_{\text{eff}} = \mathbf{J}_0$, respectively, and integrating over the variable \mathbf{r}'_2 , equation (13) becomes

$$\mathbf{W}_{12}(\mathbf{r}_1, \mathbf{r}_2) = \frac{k^2 \mathbf{J}_0}{2\pi d^2} \exp\left[\frac{ik}{2d}(\mathbf{r}_2^2 - \mathbf{r}_1^2)\right] \times \mathcal{F}\{T(\mathbf{r}'_1)\} \left[\frac{k}{d}(\mathbf{r}_1 - \mathbf{r}_2)\right], \quad (14)$$

where

$$\mathcal{F}\{T(\mathbf{r})\}[\mathbf{k}] = \frac{1}{2\pi} \int_{-\infty}^{\infty} d^2r T(\mathbf{r}) e^{i\mathbf{k}\cdot\mathbf{r}} \quad (15)$$

is the two-dimensional Fourier transform of $T(\mathbf{r})$. Since in the test path we employ a pinhole detector (see figure 3), we may naturally take it to be located at the point $\mathbf{r}_2 = \mathbf{0}$ and so equation (14) reduces to

$$\mathbf{W}_{12}(\mathbf{r}_1, \mathbf{0}) = \frac{k^2 \mathbf{J}_0}{2\pi d^2} \exp\left(-\frac{ik}{2d}\mathbf{r}_1^2\right) \mathcal{F}\{T(\mathbf{r}'_1)\} \left[\frac{k}{d}\mathbf{r}_1\right]. \quad (16)$$

Hence, using a spatially uncorrelated light source and the appropriate path-length conditions for classical ghost diffraction ($z + d$ in both arms), we have obtained the Fourier transform of the object via the notion of the effective source. We will next apply these same ideas to ghost polarimetry.

IV. GHOST POLARIMETRY

Making use of the effective source concept we present two different modifications to the classical ghost diffraction setup which are used to obtain the moduli of the Fourier transforms of each of the elements in the object's Jones matrix. Applying standard iterative methods all elements of the complex Jones matrix can then, in principle, be computed [27, 30]. We further assess separately the polarimetric image qualities of the two arrangements. One of the modifications leads to a setup which can be employed to perform polarimetry on an arbitrary

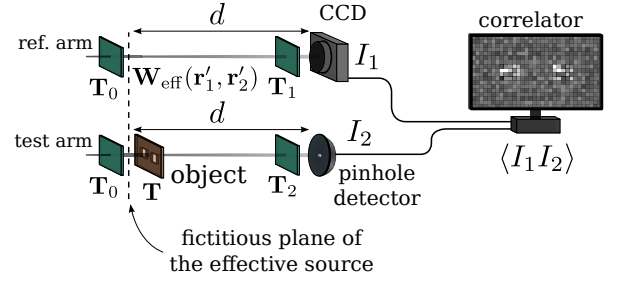


Figure 4. Ghost polarimetry configurations. The first polarizer T_0 is placed before the plane of the effective source $\mathbf{W}_{\text{eff}}(\mathbf{r}'_1, \mathbf{r}'_2)$ and affects both arms. In the reference arm another polarizer T_1 is placed before the CCD camera. In the test arm the object T is located immediately after the effective source and another polarizer T_2 is placed before the pinhole detector. The intensities I_1 and I_2 are measured at the end of the arms and correlated.

birefringent or dichroic object without a polarization-state controlled source, whereas the other gives a better image contrast in a configuration that closer resembles the conventional polarimetric setup.

A. Configurations for ghost polarimetry

For ghost polarimetry of an arbitrary planar object we modify the setup shown in figure 3 slightly. More specifically, we employ the effective source with the possibility of controlling the actual source's state of polarization with the uniform polarizer T_0 (see figure 2). In addition, spatially independent linear polarizers described by T_1 and T_2 are placed before the CCD camera in the reference arm and in front of the pinhole detector in the test arm, respectively. The object's matrix transmission function is $T(\mathbf{r}'_2)$, explicitly given by equation (2) and it can alter the state of polarization of the test beam. The simplified setup, without a detailed description of the effective source, is shown in figure 4.

In analogy with equation (13) the CSDM between the light in the two arms now becomes [see also equation (1)]

$$\mathbf{W}_{12}(\mathbf{r}_1, \mathbf{r}_2) = \iint_{-\infty}^{\infty} d^2r'_1 d^2r'_2 T_1^* \mathbf{W}_{\text{eff}}(\mathbf{r}'_1, \mathbf{r}'_2) T^T(\mathbf{r}'_2) T_2^T \times K_1^*(\mathbf{r}'_1, \mathbf{r}_1) K_2(\mathbf{r}'_2, \mathbf{r}_2), \quad (17)$$

where the integrations are in the effective source plane and the propagation kernels $K_\alpha(\mathbf{r}'_\alpha, \mathbf{r}_\alpha)$, with $\alpha \in \{1, 2\}$, are given by equation (11) with $z = d$. On inserting the CSDM of the effective source from equation (12) and the explicit forms of $K_\alpha(\mathbf{r}'_\alpha, \mathbf{r}_\alpha)$, and integrating with respect to \mathbf{r}'_2 , we obtain

$$\mathbf{W}_{12}(\mathbf{r}_1, \mathbf{r}_2) = \frac{k^2}{4\pi^2 d^2} \int_{-\infty}^{\infty} d^2r'_1 T_1^* \mathbf{J}_{\text{eff}} T^T(\mathbf{r}'_1) T_2^T$$

$$\times \exp \left\{ \frac{ik}{2d} \left[\mathbf{r}_2^2 - \mathbf{r}_1^2 - 2(\mathbf{r}_2 - \mathbf{r}_1) \cdot \mathbf{r}'_1 \right] \right\}. \quad (18)$$

To perform the polarimetric measurements, the polarizers are oriented in such a manner that the conditions $\mathbf{T}_1^* \mathbf{J}_{\text{eff}} = J_{0,ii} \mathbf{T}^i$ and $\mathbf{T}_2^T = \mathbf{T}^j$ are met, with $i, j \in \{x, y\}$ and $J_{0,ii}$ denoting a diagonal component of \mathbf{J}_0 . Specific arrangements that result in the former requirement are discussed in section IV B. Using the aforementioned conditions together with equations (3) and (18), we find that [compare with equation (14)]

$$\mathbf{W}_{12}(\mathbf{r}_1, \mathbf{r}_2) = \frac{k^2 J_{0,ii} \mathbf{T}^{ij}}{2\pi d^2} \exp \left[\frac{ik}{2d} (\mathbf{r}_2^2 - \mathbf{r}_1^2) \right] \times \mathcal{F} \{ T_{ji}(\mathbf{r}'_1) \} \left[\frac{k}{d} (\mathbf{r}_1 - \mathbf{r}_2) \right], \quad (19)$$

where $\mathcal{F} \{ T_{ji}(\mathbf{r}'_1) \} [k(\mathbf{r}_1 - \mathbf{r}_2)/d]$ is the Fourier transform of $T_{ji}(\mathbf{r}'_1)$, as defined by equation (15) and the matrix \mathbf{T}^{ij} has the element $T_{ij}^{ij} = 1$, with all the other elements being zero. With reference to figure 4 we again invoke the condition that the pinhole detector in the test arm is placed at the position $\mathbf{r}_2 = \mathbf{0}$. We then find, in analogy with equation (16), that

$$\mathbf{W}_{12}(\mathbf{r}_1, \mathbf{0}) = \frac{k^2 J_{0,ii} \mathbf{T}^{ij}}{2\pi d^2} \exp \left(-\frac{ik}{2d} \mathbf{r}_1^2 \right) \mathcal{F} \{ T_{ji}(\mathbf{r}'_1) \} \left[\frac{k}{d} \mathbf{r}_1 \right]. \quad (20)$$

Consequently, the correlation of the intensity fluctuations between the two arms is

$$\text{tr } \mathbf{W}_{12}^\dagger \mathbf{W}_{12} = \frac{k^4 J_{0,ii}^2}{4\pi^2 d^4} \left| \mathcal{F} \{ T_{ji}(\mathbf{r}'_1) \} \left[\frac{k}{d} \mathbf{r}_1 \right] \right|^2. \quad (21)$$

Note that we must separately measure the intensity fluctuation correlation for all $i, j \in \{x, y\}$.

Once the moduli of the Fourier transforms are known, the complex elements can be calculated using iterative methods [27, 30], and effects like linear birefringence and linear or circular dichroism can be observed. For scalar amplitude-only and pure phase objects [31] the iterative techniques have been demonstrated in the realm of ghost imaging [25]. Phase-contrast ghost imaging could be used for retrieval of phase-only objects [26].

B. Polarimetric qualities in the two setups

To obtain equation (21) we assumed that $\mathbf{T}_1^* \mathbf{J}_{\text{eff}} = J_{0,ii} \mathbf{T}^i$. This condition holds, for instance, when the polarizer in the reference arm is disregarded ($\mathbf{T}_1 = \mathbf{I}$), the polarizer after the source satisfies $\mathbf{T}_0 = \mathbf{T}^i$ and the actual source is polarized at an angle of 45 degrees with respect to the x axis. We call this setup case A. Another arrangement in which the condition $\mathbf{T}_1^* \mathbf{J}_{\text{eff}} = J_{0,ii} \mathbf{T}^i$ holds

is when the polarizer following the source is discarded resulting in $\mathbf{J}_{\text{eff}} = \mathbf{J}_0$, the polarizer in the reference arm satisfies $\mathbf{T}_1 = \mathbf{T}^i$, and the polarization matrix \mathbf{J}_0 of the actual source is diagonal as is true, e.g., for completely unpolarized light. This setup, which we label case B, has the important property that it would permit polarimetry without a polarization-state controlled source. We recall that in both cases A and B the polarizer in the test arm must satisfy $\mathbf{T}_2^T = \mathbf{T}^j$.

Although the main result [equation (21)] is the same in cases A and B, the polarimetric image qualities are different. There are several methods for evaluating the image quality in ghost imaging and diffraction, including multiple definitions for the visibility [1, 9, 17], the signal-to-noise ratio (SNR) [12, 32] and the contrast-to-noise ratio (CNR) [10, 11]. For a comparison between the cases A and B we assess the polarimetric quality in terms of the visibility defined as [17]

$$V \equiv \frac{\langle I_1 I_2 \rangle_{\text{max}} - \langle I_1 I_2 \rangle_{\text{min}}}{\langle I_1 I_2 \rangle_{\text{max}} + \langle I_1 I_2 \rangle_{\text{min}}}, \quad (22)$$

where the subscript max denotes the average over the bright area of the image and the subscript min stands for the average over the dark area. Using equation (9) we obtain

$$V = \frac{[\text{tr } \mathbf{W}_{12}^\dagger \mathbf{W}_{12}]_{\text{max}} - [\text{tr } \mathbf{W}_{12}^\dagger \mathbf{W}_{12}]_{\text{min}}}{2 \text{tr } \mathbf{W}_{11} \text{tr } \mathbf{W}_{22} + [\text{tr } \mathbf{W}_{12}^\dagger \mathbf{W}_{12}]_{\text{max}} + [\text{tr } \mathbf{W}_{12}^\dagger \mathbf{W}_{12}]_{\text{min}}}. \quad (23)$$

The visibility thus depends not only on the correlation of the intensity fluctuations between the reference and test arms ($\text{tr } \mathbf{W}_{12}^\dagger \mathbf{W}_{12}$) but also on the background term in ghost imaging, i.e., the product of the intensities measured in the reference ($\text{tr } \mathbf{W}_{11}$) and test ($\text{tr } \mathbf{W}_{22}$) arms. As already noted, the CSDM \mathbf{W}_{12} between the light in the reference and test arms is the same in the two cases A and B, since each case leads to equation (20) and subsequently equation (21) is obtained.

Also the intensities in the reference arm are identical in both cases A and B, as moving the polarizer from the vicinity of the source to in front of the reference arm detector does not change anything for that arm. The explicit form of the CSDM for the reference arm is calculated in appendix A, equation (A5). Its trace then is

$$\text{tr } \mathbf{W}_{11} = J_{0,ii}. \quad (24)$$

The average intensity in the reference arm is independent of transverse position across the detector.

However, in the test arm the intensities are slightly different for the two cases. In case A the polarizer \mathbf{T}_0 placed directly after the source can control the polarization state of the light that goes into the reference arm detector as well as of the light that traverses the object in the test arm. In this situation we obtain, from equation (A7),

$$\text{tr } \mathbf{W}_{22} = \frac{k^2 J_{0,ii}}{4\pi^2 d^2} \int_{-\infty}^{\infty} d^2 r'_1 |T_{ji}(\mathbf{r}'_1)|^2. \quad (25)$$

On the other hand, in case B, in which the source is fixed and the polarizer is in front of the reference arm detector, the light interacting with the object has not been filtered from unnecessary polarization states. From equation (A8) we now have

$$\begin{aligned} \text{tr } \mathbf{W}_{22} &= \frac{k^2}{4\pi^2 d^2} \int_{-\infty}^{\infty} d^2 r'_1 \\ &\times \left(J_{0,xx} |T_{ix}(\mathbf{r}'_1)|^2 + J_{0,yy} |T_{iy}(\mathbf{r}'_1)|^2 \right), \quad (26) \end{aligned}$$

The average intensity in the test arm [equations (25) and (26)] likewise is independent of transverse position, albeit we need it only at the location of the pinhole detector.

The visibility V for case A can be calculated using equations (21)–(25). For case B the last equation is replaced by the intensity given by equation (26). Comparing the two options we note that in case B the intensity in the test arm is larger if a similar source is used and when all the object's transmission function's elements are nonzero, i.e., $|T_{ij}(\mathbf{r}'_1)| > 0$ for all $i, j \in \{x, y\}$. From the form of equation (23) we may then conclude that this results in lower visibility when compared to case A. However, we emphasize that case B can be used in novel polarimetric measurements, due to the fact that the classical source's state of polarization does not need to be controlled.

V. CONCLUSIONS

By a modification to the conventional ghost diffraction experiment with classical spatially incoherent light, a method for polarimetry by ghost imaging has been introduced. Using the Jones matrix formalism to analyze an electromagnetic ghost diffraction setup with polarization-dependent optical elements, we have shown that adding two uniform linear polarizers permits one to measure the Jones matrix of an arbitrary birefringent or dichroic object. The first polarizer can be placed in front of the reference arm detector to enable polarimetry without controlling the state of polarization of the light source. However, higher polarimetric quality in terms of image visibility is achieved when the first polarizer is placed immediately after the source. The second polarizer has to be located between the object and the test arm detector to discriminate how the object changes the different states of polarization of the illumination. The general method presented in this work, called ghost polarimetry, enables the assessment of the polarimetric properties of spatially dependent objects in novel ways merely by means of intensity correlations.

We have also demonstrated that the use of the effective source concept greatly simplifies the calculations related to both scalar and electromagnetic ghost diffraction setups. The effective source can be seen as a useful mathematical tool for the analysis of a wide range

of ghost imaging and diffraction arrangements. It was shown that for sufficiently wide beams the effective source retains the spatially completely incoherent nature of the original source.

ACKNOWLEDGMENTS

Part of this work was done while HK was working with Aalto University. HK acknowledges support from the Väisälä Fund granted by the Finnish Academy of Science and Letters. This research was also supported by the Academy of Finland (projects 272692, 268480 and 268705) and by the Japan Society for the Promotion of Science (KAKENHI 23656054 and 25390104).

Appendix A: Placement of the optical elements

In ghost imaging, such as the setup depicted in figure 4, the information is encoded in the correlation of the intensity fluctuations, i.e., in $\text{tr } \mathbf{W}_{12}^\dagger \mathbf{W}_{12}$. For the discussion in section A 1, the essential part is the influence of the matrices \mathbf{T}_1 , \mathbf{J}_{eff} , $\mathbf{T}(\mathbf{r}'_1)$ and \mathbf{T}_2 [see equation (18)] on $\text{tr } \mathbf{W}_{12}^\dagger \mathbf{W}_{12}$. We need to measure the individual elements of $\mathbf{T}(\mathbf{r}'_1)$. Using two different objects as an example, we show that leaving out the polarizer between the object and the pinhole detector ($\mathbf{T}_2 = \mathbf{I}$), or leaving out both the polarizer after the source ($\mathbf{J}_{\text{eff}} = \mathbf{J}_0$) and the polarizer before the CCD in the reference arm ($\mathbf{T}_1 = \mathbf{I}$), will make it impossible to distinguish between the objects.

In section A 2 we present details of the two cases in which the first polarizer is located in place of either \mathbf{T}_0 or \mathbf{T}_1 and the second polarizer is represented by \mathbf{T}_2 . We examine each case separately to find what kind of source is appropriate for the polarimetric imaging and calculate the CSDMs for the individual arms. The CSDMs are used in the discussion related to polarimetric quality in section IV B.

1. Necessary polarizers

With the goal of showing that leaving out certain polarizers leads to an unsuccessful measurement, first we consider the case in which there is no polarizer after the source or in front of the reference arm detector. In this case $\mathbf{J}_{\text{eff}} = \mathbf{J}_0$ and $\mathbf{T}_1 = \mathbf{I}$. The polarization matrix is Hermitian and non-negative definite and is thus diagonalizable with a unitary transformation \mathbf{U} and non-negative eigenvalues J_1 and J_2 . Let us perform the same transformation also to the other matrices appearing in \mathbf{W}_{12} , i.e.,

$$\mathbf{J}'_0 = \mathbf{U} \mathbf{J}_0 \mathbf{U}^\dagger = \begin{pmatrix} J_1 & 0 \\ 0 & J_2 \end{pmatrix}, \quad (\text{A1a})$$

$$\mathbf{T}'^T(\mathbf{r}'_1) = \mathbf{U} \mathbf{T}^T(\mathbf{r}'_1) \mathbf{U}^\dagger, \quad (\text{A1b})$$

$$\mathbf{T}_2^T = \mathbf{U}\mathbf{T}_2^T\mathbf{U}^\dagger. \quad (\text{A1c})$$

We present two example objects that can not be distinguished from each other. The first one is represented by a diagonal matrix $\mathbf{T}'(\mathbf{r}'_1)$ with the elements $T'_{xx}(\mathbf{r}'_1) = g(\mathbf{r}'_1)$ and $T'_{yy}(\mathbf{r}'_1) = \kappa g(\mathbf{r}'_1)$, where $\kappa \equiv J_1/J_2$ and $g(\mathbf{r}'_1)$ is a Fourier-transformable complex function. The second object has the non-zero elements $T'_{xy}(\mathbf{r}'_1) = -\kappa g(\mathbf{r}'_1)$ and $T'_{yx}(\mathbf{r}'_1) = g(\mathbf{r}'_1)$ (obtained by placing a $\pi/2$ rotator after the first object). Combining equations (18) and (A1) together with the conditions $\mathbf{J}_{\text{eff}} = \mathbf{J}_0$ and $\mathbf{T}_1 = \mathbf{I}$, we obtain

$$\text{tr } \mathbf{W}_{12}^\dagger \mathbf{W}_{12} = \frac{J_1^2 k^4}{4\pi^2 d^4} \left| \mathcal{F} \{g(\mathbf{r}'_1)\} \left[\frac{k}{d} (\mathbf{r}_1 - \mathbf{r}_2) \right] \right|^2 \text{tr } \mathbf{T}_2^* \mathbf{T}_2^T, \quad (\text{A2})$$

where $\mathcal{F}\{g(\mathbf{r}'_1)\}[k(\mathbf{r}_1 - \mathbf{r}_2)/d]$ is defined by equation (15). This result was acquired using the invariance of the trace under unitary transformations and the intermediate result given by $\text{tr } \mathbf{T}_2^* \mathbf{T}'^*(\mathbf{r}'_1) \mathbf{J}_0^2 \mathbf{T}'^T(\mathbf{r}'_1) \mathbf{T}_2^T = J_1^2 g^*(\mathbf{r}'_1) g(\mathbf{r}'_1) \text{tr } \mathbf{T}_2^* \mathbf{T}_2^T$. Equation (A2) holds for both example objects and we can thus conclude that by varying \mathbf{T}_2 (or \mathbf{T}'_2) we are not able to make a distinction between the two cases, although their Jones matrices are different.

Similar reasoning applies when the effective source and the polarizer in front of the reference arm detector are variable but the test arm detector lacks a polarizer ($\mathbf{T}_2 = \mathbf{I}$). Using either of the example objects presented above, in this situation we have [see equation (18)]

$$\text{tr } \mathbf{W}_{12}^\dagger \mathbf{W}_{12} = \frac{k^4}{4\pi^2 d^4} \left| \mathcal{F} \{g(\mathbf{r}'_1)\} \left[\frac{k}{d} (\mathbf{r}_1 - \mathbf{r}_2) \right] \right|^2 \times (B_{xx} + \kappa^2 B_{yy}), \quad (\text{A3})$$

where B_{ii} , $i \in \{x, y\}$, is the diagonal component of the (generally non-diagonal) matrix $\mathbf{B} \equiv \mathbf{J}_{\text{eff}}^\dagger \mathbf{T}_1^T \mathbf{T}_1^* \mathbf{J}_{\text{eff}}$ and we used $\text{tr } \mathbf{T}^*(\mathbf{r}'_1) \mathbf{B} \mathbf{T}^T(\mathbf{r}'_1) = g^*(\mathbf{r}'_1) g(\mathbf{r}'_1) (B_{xx} + \kappa^2 B_{yy})$. Since the result is the same for both objects, no matter how \mathbf{J}_{eff} and \mathbf{T}_1 are chosen, the objects are indistinguishable when $\mathbf{T}_2 = \mathbf{I}$.

In practice this means that ghost polarimetry is not possible when the polarizer between the object and the test arm detector is left out ($\mathbf{T}_2 = \mathbf{I}$), or if that optical element is the only polarizer in the ghost imaging arrangement ($\mathbf{J}_{\text{eff}} = \mathbf{J}_0$ and $\mathbf{T}_1 = \mathbf{I}$). This is analogous to the polarimetric analysis performed by the conventional device shown in figure 1 in the sense that leaving out the polarizer on either side of the object would result in an unsuccessful measurement.

2. Example measurements

In section IV B two arrangements for obtaining the polarization properties of the object were introduced. As

shown in section IV A, the intensity fluctuation correlation ($\text{tr } \mathbf{W}_{12}^\dagger \mathbf{W}_{12}$) is the same in both cases. However, the requirements on the source are slightly different and are discussed in the following subsections. The CSDMs of the reference (\mathbf{W}_{11}) and test (\mathbf{W}_{22}) arms needed to obtain the background term in equation (23) are evaluated. They are used to assess the polarimetric quality in section IV B.

In the arrangement labeled case A, the polarizer in front of the reference arm detector is omitted ($\mathbf{T}_1 = \mathbf{I}$) and we choose $\mathbf{T}_0 = \mathbf{T}^i$ for the polarizer after the source and thus $\mathbf{J}_{\text{eff}} = \mathbf{T}^i \mathbf{J}_0 \mathbf{T}^i$. In case B, the polarizer is moved from after the source to in front of the reference arm detector and we have $\mathbf{J}_{\text{eff}} = \mathbf{J}_0$ and $\mathbf{T}_1 = \mathbf{T}^i$. In both cases the test arm has the polarizer $\mathbf{T}_2 = \mathbf{T}^j$.

a. Case A: Polarizer after the source

In this case, the effective source's polarization matrix, $\mathbf{J}_{\text{eff}} = \mathbf{T}_0^* \mathbf{J}_0 \mathbf{T}_0^T$, is proportional to $\mathbf{T}_0 = \mathbf{T}^i$ when \mathbf{J}_0 is not polarized perpendicular to \mathbf{T}^i . This has to hold for $i \in \{x, y\}$ and thus a source which is completely polarized in either the x or y direction cannot be used. In order to obtain the same intensity for both orientations ($i \in \{x, y\}$) of the polarizer \mathbf{T}_0 , the source should be either completely unpolarized, (partially) circularly polarized, or (partially) linearly polarized at ± 45 degrees from the x axis.

To calculate the CSDM related to the reference arm (\mathbf{W}_{11}), we use a source slightly modified from equation (12), with the Dirac delta function replaced by a normalized coherence function that has the property $\gamma(\mathbf{0}) = 1$, thus leading to the CSDM $\mathbf{W}_{\text{eff}}(\mathbf{r}'_1, \mathbf{r}'_2) = \mathbf{J}_{\text{eff}} \gamma(\mathbf{r}'_2 - \mathbf{r}'_1)$. Using a different source here is permitted for the qualitative visibility comparison between the two cases we perform in section IV B. The γ source together with equations (1), (10), and (11) produces the reference arm CSDM

$$\mathbf{W}_{11}(\mathbf{r}_1, \mathbf{r}_1) = \frac{k^2 \mathbf{T}_1^* \mathbf{J}_{\text{eff}} \mathbf{T}_1^T}{4\pi^2 d^2} \iint_{-\infty}^{\infty} d^2 r'_1 d^2 r'_2 \gamma(\mathbf{r}'_2 - \mathbf{r}'_1) \times \exp \left\{ \frac{ik}{2d} \left[\mathbf{r}'_2^2 - \mathbf{r}'_1^2 - 2(\mathbf{r}'_2 - \mathbf{r}'_1) \cdot \mathbf{r}_1 \right] \right\}. \quad (\text{A4})$$

With the change of variables $\Delta \mathbf{r}' = \mathbf{r}'_2 - \mathbf{r}'_1$ and $\mathbf{R}' = (\mathbf{r}'_1 + \mathbf{r}'_2)/2$, the integration with respect to \mathbf{R}' becomes proportional to the delta function $\delta(k\Delta \mathbf{r}'/d)$. After scaling the delta function, integrating over it and using the property $\gamma(\mathbf{0}) = 1$, we have

$$\mathbf{W}_{11}(\mathbf{r}_1, \mathbf{r}_1) = \mathbf{T}_1^* \mathbf{J}_{\text{eff}} \mathbf{T}_1^T = J_{0,ii} \mathbf{T}^i \quad (\text{A5})$$

with $i \in \{x, y\}$. The latter form in equation (A5) follows from $\mathbf{J}_{\text{eff}} = \mathbf{T}^i \mathbf{J}_0 \mathbf{T}^i = J_{0,ii} \mathbf{T}^i$ and $\mathbf{T}_1 = \mathbf{I}$.

To compute the CSDM of the test arm (\mathbf{W}_{22}) we return to the delta-correlated source. Using equations (1), (10),

(11) and (12) we obtain (after integration over \mathbf{r}'_2)

$$\mathbf{W}_{22}(\mathbf{r}_2, \mathbf{r}_2) = \frac{k^2}{4\pi^2 d^2} \int_{-\infty}^{\infty} d^2 r'_1 \mathbf{T}_2^* \mathbf{T}^*(\mathbf{r}'_1) \mathbf{J}_{\text{eff}} \mathbf{T}^T(\mathbf{r}'_1) \mathbf{T}_2^T. \quad (\text{A6})$$

Again employing $\mathbf{J}_{\text{eff}} = J_{0,ii} \mathbf{T}^i$ the test arm CSDM becomes

$$\mathbf{W}_{22}(\mathbf{r}_2, \mathbf{r}_2) = \frac{k^2 J_{0,ii} \mathbf{T}^j}{4\pi^2 d^2} \int_{-\infty}^{\infty} d^2 r'_1 |T_{ji}(\mathbf{r}'_1)|^2 \quad (\text{A7})$$

with $i, j \in \{x, y\}$, since $\mathbf{T}^j \mathbf{T}(\mathbf{r}'_1) \mathbf{T}^i = T_{ji}(\mathbf{r}'_1) \mathbf{T}^{ji}$. The traces of equations (A5) and (A7) are used to obtain equations (24) and (25).

b. Case B: Polarizer in front of the reference arm detector

When the first polarizer is placed in front of the reference arm detector the matrix $\mathbf{T}_1^* \mathbf{J}_0$ is proportional to $\mathbf{T}_1 = \mathbf{T}^i$ when \mathbf{J}_0 is diagonal. [This proportionality is required to find the main imaging result, equation (21).] To obtain equal intensities for both field components of the source, the light needs to be completely unpolarized. Light which is partially linearly polarized along either the x or y axis is also sufficient but will result in a lower intensity source for one of the measurements when $i \in \{x, y\}$ is varied.

Using equation (A6) and the constraints $\mathbf{J}_{\text{eff}} = \mathbf{J}_0$ and $\mathbf{T}_2 = \mathbf{T}^j$, we note that the term $J_{0,ii} |T_{ji}(\mathbf{r}'_1)|^2$ in equation (A7) is replaced by $J_{0,xx} |T_{jx}(\mathbf{r}'_1)|^2 + J_{0,yy} |T_{jy}(\mathbf{r}'_1)|^2$. Thus the CSDM for the test arm is

$$\mathbf{W}_{22}(\mathbf{r}_2, \mathbf{r}_2) = \frac{k^2 \mathbf{T}^j}{4\pi^2 d^2} \int_{-\infty}^{\infty} d^2 r'_1 \times \left(J_{0,xx} |T_{jx}(\mathbf{r}'_1)|^2 + J_{0,yy} |T_{jy}(\mathbf{r}'_1)|^2 \right). \quad (\text{A8})$$

Taking the trace of equation (A8) results in equation (26).

-
- [1] A. Gatti, E. Brambilla, and L. Lugiato, in *Progress in Optics*, Vol. 51, edited by E. Wolf (Elsevier, 2008) pp. 251–348
- [2] B. I. Erkmen and J. H. Shapiro, *Adv. Opt. Photon.* **2**, 405 (2010)
- [3] A. Gatti, E. Brambilla, M. Bache, and L. Lugiato, *Phys. Rev. A* **70**, 013802 (2004)
- [4] A. Gatti, E. Brambilla, M. Bache, and L. Lugiato, *Phys. Rev. Lett.* **93**, 093602 (2004)
- [5] A. Valencia, G. Scarcelli, M. D'Angelo, and Y. Shih, *Phys. Rev. Lett.* **94**, 063601 (2005)
- [6] F. Ferri, D. Magatti, A. Gatti, M. Bache, E. Brambilla, and L. Lugiato, *Phys. Rev. Lett.* **94**, 183602 (2005)
- [7] A. Gatti, M. Bache, D. Magatti, E. Brambilla, F. Ferri, and L. A. Lugiato, *J. Mod. Opt.* **53**, 739 (2006)
- [8] V. Torres-Company, H. Lajunen, J. Lancis, and A. T. Friberg, *Phys. Rev. A* **77**, 043811 (2008)
- [9] D.-Z. Cao, J. Xiong, S.-H. Zhang, L.-F. Lin, L. Gao, and K. Wang, *Appl. Phys. Lett.* **92**, 201102 (2008)
- [10] K. W. C. Chan, M. N. O'Sullivan, and R. W. Boyd, *Opt. Express* **18**, 5562 (2010)
- [11] H. Kellock, T. Setälä, T. Shirai, and A. T. Friberg, *J. Opt. Soc. Am. A* **29**, 2459 (2012)
- [12] F. Ferri, D. Magatti, L. Lugiato, and A. Gatti, *Phys. Rev. Lett.* **104**, 253603 (2010)
- [13] J. H. Shapiro, *Phys. Rev. A* **78**, 061802 (2008)
- [14] Y. Bromberg, O. Katz, and Y. Silberberg, *Phys. Rev. A* **79**, 053840 (2009)
- [15] H.-C. Liu, D.-S. Guan, L. Li, S.-H. Zhang, and J. Xiong, *Opt. Commun.* **283**, 405 (2010)
- [16] Z. Tong, Y. Cai, and O. Korotkova, *Opt. Commun.* **283**, 3838 (2010)
- [17] T. Shirai, H. Kellock, T. Setälä, and A. T. Friberg, *Opt. Lett.* **36**, 2880 (2011)
- [18] A. F. Abouraddy, J. Toussaint, Kimani C., A. V. Sergienko, B. E. A. Saleh, and M. C. Teich, *Opt. Lett.* **26**, 1717 (2001)
- [19] A. F. Abouraddy, J. Toussaint, Kimani C., A. V. Sergienko, B. E. A. Saleh, and M. C. Teich, *J. Opt. Soc. Am. B* **19**, 656 (2002)
- [20] J. Toussaint, Kimani C., G. Di Giuseppe, K. J. Bycenski, A. V. Sergienko, B. E. A. Saleh, and M. C. Teich, *Phys. Rev. A* **70**, 023801 (2004)
- [21] C. Brosseau, *Fundamentals of Polarized Light: A Statistical Optics Approach* (Wiley, 1985)
- [22] B. E. A. Saleh and M. C. Teich, *Fundamentals of Photonics*, 2nd ed. (Wiley, 2007)
- [23] Y. Cai and S.-Y. Zhu, *Opt. Lett.* **29**, 2716 (2004)
- [24] J. Cheng and S. Han, *Phys. Rev. Lett.* **92**, 093903 (2004)
- [25] M. Zhang, Q. Wei, X. Shen, Y. Liu, H. Liu, J. Cheng, and S. Han, *Phys. Rev. A* **75**, 021803 (2007)
- [26] T. Shirai, T. Setälä, and A. T. Friberg, *Phys. Rev. A* **84**, 041801(R) (2011)
- [27] T. Shirai, H. Kellock, T. Setälä, and A. T. Friberg, *J. Opt. Soc. Am. A* **29**, 1288 (2012)
- [28] L. Mandel and E. Wolf, *Optical Coherence and Quantum Optics* (Cambridge University, 1995)
- [29] J. W. Goodman, *Introduction to Fourier Optics*, 3rd ed. (Roberts & Company, 2005)
- [30] W. McBride, N. L. O'Leary, and L. J. Allen, *Phys. Rev. Lett.* **93**, 233902 (2004)
- [31] V. Elser, *J. Opt. Soc. Am. A* **20**, 40 (2003)
- [32] G. Brida, M. Chekhova, G. Fornaro, M. Genovese, E. Lopaeva, and I. Berchera, *Phys. Rev. A* **83**, 063807 (2011)